Derivation of risk-targeted maps for Italy based on a simplified approach

Athanasios Gkimprixis[a], Enrico Tubaldi[a] and John Douglas[a]
[a] *Department of Civil and Environmental Engineering, University of Strathclyde, Glasgow, UK.*

Keywords: Risk targeting, seismic design, behaviour factor, hazard maps, probabilistic seismic analysis

ABSTRACT
In the recent years, risk-targeting has emerged as an innovative way of designing structures. The advantage of this approach compared to the one based on uniform-hazard spectra is that it enables direct control of the structural performance due to potential future earthquakes. Alternative methods have been proposed for applying risk-targeting in practice. Among these, one based on the use of risk-targeted behaviour factors (RTBFs) has been recently considered for the development of future versions of Eurocode 8. This study shows the results of the application of the RTBF approach for the definition of risk-targeted maps for Italy.

1 INTRODUCTION

The design of structures according to current seismic codes is based on the use of a uniform hazard spectrum (UHS) divided by a behaviour factor relevant to the structural system under study. This approach has been shown to result in inconsistent values of risk, which vary with the vibration period of the structure, and also for the same structure located in areas of different hazard (see e.g. Iervolino et al. 2017).

As a result, research efforts focus now on the development of alternative techniques to control the seismic structural performance in the assessment and design stage (Fragiadakis and Papadrakakis 2008; Barbato and Tubaldi 2013; Gidaris and Taflanidis 2015; Castaldo et al. 2017; Altieri et al. 2018; Franchin et al. 2018). Simplified methods have been proposed, as well, based on the probabilistic framework outlined in Kennedy and Short (1994) and Cornell (1996), which led to the development of the SAC-FEMA framework (Cornell et al. 2002) for seismic design of steel moment resisting frames, enhanced by others (e.g. Lupoi et al. 2002; Vamvatsikos 2013). This framework introduces some simplifying assumptions to allow for a closed-form approximation of the mean annual frequency (MAF) of limit state exceedance. Based on the concepts and procedures developed by these methods, Fajfar and Dolšek (2012) introduced a practice-oriented approach for seismic risk assessment. This method employs pushover analysis instead of more time consuming dynamic analyses for response assessment and considers a default value of the dispersion to account for record-to-record variability effects. Moreover, Žižmond and Dolšek (2017) developed the concept of risk-targeted behaviour factors (RTBFs), as a means to control the risk of exceedance of different limit states by the structure during the design procedure. Vamvatsikos and Aschheim (2016) introduced the concept of yield frequency spectra, enabling the direct design of a structure subject to a set of performance objectives. Such spectra can be used to provide the risk-targeted yield strength of a system that satisfies an acceptable ductility response level.

In the United States, following the work of Luco et al. (2007), the concept of risk-targeting has emerged. This aims to define ground motion maps adopting a “uniform risk” rather than a “uniform hazard” concept. With this approach, the seismic uniform-hazard ground motion maps are modified to obtain more consistent levels of the collapse probability across the country. While risk targeted design maps have been already implemented in American seismic design codes (see Luco et al., 2015), they have not yet been introduced in practice in Europe (Douglas and Gkimprixis 2018), where the implementation of probabilistic behaviour factor concepts in Eurocode 8 is still under consideration (Fajfar 2018).

This article is based on a previous work of the authors (Gkimprixis et al. 2019), where different risk-targeting techniques are presented and compared. Herein, one of the techniques is summarised, namely the risk-targeted behaviour factor (RTBF) approach. This technique is based on the work of Kennedy and Short (1994) and Cornell (1996). Using a different hazard input than the one in the aforementioned work, the RTBF technique is applied to develop risk targeted design maps for Italy.

2 THE RISK-TARGETED BEHAVIOUR FACTOR (RTBF) APPROACH

In risk-targeting, the risk is defined as the MAF of limit state exceedance λ_{LS} and can be estimated through the total probability theorem (e.g. Benjamin and Cornell 1970) as:

$$\lambda_{LS} = \int P\left(C|S_a\right)\left|dH(S_a)\right| \tag{1}$$

where the symbol "d" denotes the differentiation operator, $H\left(S_a\right)$ is the hazard curve, providing the MAF of exceeding S_a, from PSHA (McGuire 2008; Baker 2015), and $P\left(C|S_a\right)$ corresponds to the conditional probability of exceeding the limit state under an earthquake with intensity S_a .This probability is given by:

$$P\left(C|S_a\right) = P\left[S_a > S_a^c\right] \tag{2}$$

where S_a^c is the limit state capacity, i.e., the value of the spectral acceleration causing the exceedance of the limit state. It is noteworthy that this probability must account for the so called record-to-record variability effects and the effect of the uncertainty in the structural capacity, as done in Cornell (1996).

Kennedy and Short (1994) and Cornell (1996), developed a simple and practice-oriented approach for estimating the seismic risk of a structural system, which can be conveniently used for designing the system's strength for a target reliability level. In particular, a closed-form expression of the MAF of failure of the system λ_{LS} can be obtained by introducing a series of simplifying assumptions. In the following, the limit state definition is based on a measure of the global ductility of the system, μ . This entails defining explicitly a yield condition and an ultimate or "failure" condition, which can be kinematically related to each other. Different choices can be made when defining these conditions, which may require identifying an elasto-plastic single-degree-of-freedom (SDOF) system equivalent to the structure under investigation (Cornell 1996, Aschheim, 2002). Hereinafter, the condition of "failure" corresponds to the ductility demand μ_d imposed by the earthquake exceeding the ductility capacity μ_c. The corresponding MAF of limit state exceedance is denoted hereinafter as λ_c, to highlight the fact that failure corresponds to exceedance of the ductility capacity.

An important assumption concerns the seismic hazard, $H\left(S_a\right)$, which is represented by a linear equation in log-log space:

$$H\left(S_a\right) = k_0 \cdot S_a^{-k_1} \tag{3}$$

The limit state capacity S_a^c, can be expressed in terms of the following product (e.g. Cornell 1996):

$$S_a^c = q_{\mu_c} \cdot S_a^y \cdot \varepsilon_{\mu_c} \tag{4}$$

where S_a^y is the spectral acceleration inducing yielding of the system, q_{μ_c} is the ductility-dependent contribution of the behaviour factor, denoting the factor by which a specific acceleration time history capable of causing incipient first yield must be scaled up to produce a ductility demand equal to the median capacity $\hat{\mu}_c$ and ε_{μ_c} is a lognormal random variable with unit mean and lognormal standard deviation β_{μ_c} that captures the variability of the ductility capacity in spectral acceleration terms.

S_a^y and q_{μ_c} are also generally random variables, due to record-to-record variability effects. Cornell (1996) assumes that these two random variables follow a lognormal distribution, with median values equal to $\hat{S}_a^y$ and $\hat{q}_{\mu_c}$ respectively, and lognormal standard deviation, or dispersion, $\beta_{S_a^y}$ and $\beta_{q_{\mu_c}}$. In the case of a deterministic SDOF system, if the pseudo-spectral acceleration is used as the IM, then the yield acceleration has zero dispersion, i.e., $\beta_{S_a^y}$ =0, because it is directly related to the yield displacement u_y through the relation $S_a^y = \omega^2 \cdot u_y$. This is generally not true in the more general case of multiple-degrees-of-freedom systems, due to the influence of higher modes of vibration (Luco and Cornell 2007).

The product of lognormal random variables is also a lognormal random variable. Thus, the limit state capacity S_a^c follows a lognormal distribution with median $\hat{S}_a^c = \hat{q}_{\mu_c} \cdot \hat{S}_a^y$ and lognormal standard deviation $\beta = \sqrt{{\beta_{S_a^y}}^2 + {\beta_{q_{\mu_c}}}^2 + {\beta_{\mu_c}}^2}$.

Therefore, under the aforementioned assumptions, the MAF of limit state exceedance, can be expressed as (Kennedy and Short 1994, Cornell 1996):

$$\lambda_c = H\left(\hat{S}_a^c\right)\cdot e^{0.5\cdot(k_1\cdot\beta)^2} = k_0\cdot\left(\hat{S}_a^y\right)^{-k_1}\cdot\hat{q}_{\mu_c}{}^{-k_1}\cdot e^{0.5\cdot(k_1\cdot\beta)^2} \quad (5)$$

This equation can be inverted to find the median value of $\hat{S}_a^y$ corresponding to a prefixed value of the MAF of failure. In order to exploit this formulation for design purposes, it is better to introduce the overstrength of the system q_s, similarly to Žižmond and Dolšek (2017). This overstrength is defined as the ratio between the spectral acceleration at yield of the system and the design spectral acceleration S_a^d (Kappos 1999):

$$q_s = \hat{S}_a^y / S_a^d \quad (6)$$

Substituting Equation (6) into Equation (5) gives the following expression of the MAF of failure, where now the dependence on the design spectral acceleration is made explicit:

$$\lambda_c\left(S_a{}^d\right) = H\left(S_a{}^d\right)\cdot f_{hc} \quad (7)$$

where $f_{hc} = \hat{q}_{\mu_c}{}^{-k_1}\cdot q_s{}^{-k_1}\cdot e^{0.5\cdot(k_1\cdot\beta)^2}$.

A risk curve $\lambda_c\left(S_a{}^d\right)$ can be built by plotting the values of λ_c against the values of the design spectral acceleration $S_a{}^d$. Figure 1a plots and compares the relation between the hazard curve $H\left(S_a{}^d\right)$ and the risk curve $\lambda_c\left(S_a{}^d\right)$. The hazard curve for $S_a{}^d$ is obtained by linearizing the site hazard curve (more insight into the effect of the linearization is given in Gkimprixis et al. 2019, Section 3.1). If the hazard curve is linear, then so is the risk curve by virtue of Equation 7. Figure 1a also plots the yield curve $\lambda_y\left(S_a{}^d\right)$ corresponding to the MAF of yielding for a system designed with a spectral acceleration $S_a{}^d$. This can be obtained by setting $\hat{\mu}_c$ =1, which also corresponds to $\hat{q}_{\mu_c}$ =1 in Equation.7:

$$\lambda_y\left(S_a{}^d\right) = H\left(S_a{}^d\right)\cdot f_{hy} \quad (8)$$

where $f_{hy} = q_s{}^{-k_1}\cdot e^{0.5\cdot(k_1\cdot\beta)^2}$.

Again, if the hazard curve is linear, then so is the risk and yield curves by virtue of Equation (7) and Equation (8).

The design pseudo-spectral acceleration corresponding to a target value of the MAF of collapse λ_c for a system with median ductility capacity $\hat{\mu}_c$, can be obtained from Equation (7) as:

$$S_a^d = \frac{\hat{S}_a^c}{\hat{q}_{\mu_c}\cdot q_s} = \frac{1}{\hat{q}_{\mu_c}\cdot q_s}\cdot\left(\frac{k_0}{\lambda_c}\right)^{1/k_1}\cdot e^{0.5\cdot k_1\cdot\beta^2} \quad (9)$$

Using this equation one can obtain the uniform-risk design spectrum for a site, by plotting the values of S_a^d against T for a given ductility capacity and MAF of collapse. In contrast to the inelastic spectrum in design codes, this spectrum provides a consistent level of the risk of failure for systems with different vibration periods. Figure 1b shows the uniform hazard spectrum (UHS), the corresponding uniform risk spectrum (URS) and the yield spectrum (YS), derived for the target MAF of exceedance of 1/2500, assuming q_s =2 and a ductility level of 4, for an example site (see following section). The values of these spectral ordinates for T=1s can be obtained by intersecting the hazard and risk curves with a horizontal line at target MAF of 1/2500 in Figure 1a.

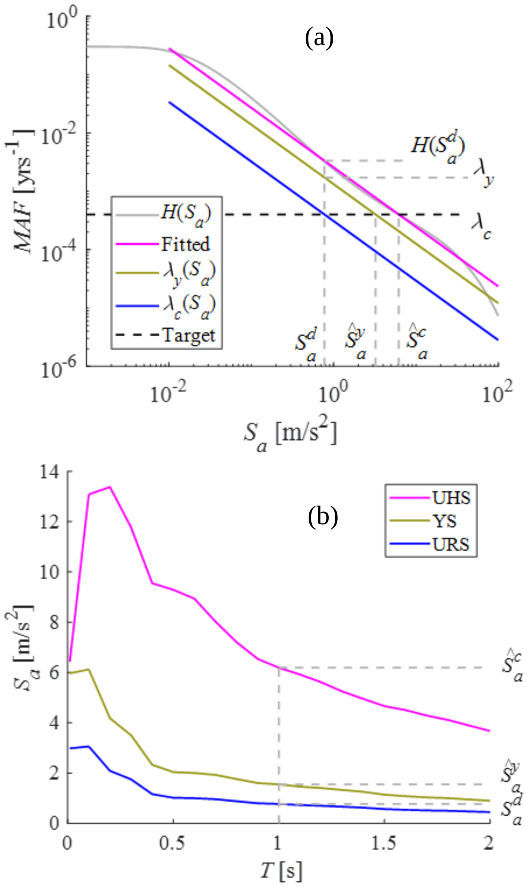

Figure 1. (a) Risk, yield and hazard curves for a system with T=1s; (b) uniform hazard spectrum (UHS), uniform risk spectrum (URS) and yield spectrum (YS) for a MAF of exceedance of 1/2500 (after Gkimprixis et al. 2019).

The seismic design input is usually expressed in regulations in terms of a UHS for a given reference MAF of its exceedance, λ_{ref} , which does not necessarily coincide with the target MAF of limit state exceedance λ_c . Let $S_a^{ref} = \left(\frac{k_0}{\lambda_{ref}}\right)^{1/k_1}$ denote the spectral ordinate of the system with period *T*, obtained by inverting the hazard curve of S_a for the MAF of exceedance λ_{ref} . After dividing S_a^{ref} by S_a^d the risk-targeted behaviour factor (Žižmond and Dolšek 2017; Fajfar 2018) is then obtained:

$$q = \frac{S_a^{ref}}{S_a^d} = \frac{\hat{q}_{\mu_c} \cdot q_s}{\gamma_{IM}} \tag{10}$$

where $\gamma_{IM} = \frac{\hat{S}_a^c}{S_a^{ref}} = \left(\frac{\lambda_{ref}}{\lambda_c}\right)^{1/k_1} \cdot e^{0.5 \cdot k_1 \cdot \beta^2}$ is a factor accounting for the difference between the MAF of the seismic design input and the target MAF of collapse. It is useful to note that for a given S_a^{ref} this equation can provide S_a^d without the need to estimate the parameter k_0.

To summarize, the spectral ordinate S_a^{ref} corresponding to the elastic response spectrum and the MAF of exceedance λ_{ref} , should be divided by q to design a system reaching the target performance, i.e., a MAF of collapse equal to λ_c . This factor is equal to the product of three components: q_s accounting for the system's overstrength, $\hat{q}_{\mu_c}$ for the system's ductility capacity, and $\gamma_{IM} = \frac{\hat{S}_a^c}{S_a^{ref}}$ for the difference in the MAF of exceedance of the input and of collapse. Figure 2 illustrates the relation between the spectral ordinates and the various components of *q* in the acceleration-displacement response spectrum plane.

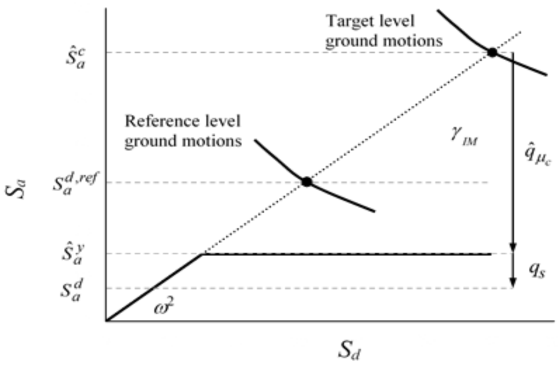

Figure 2. Relation between the spectral ordinates and the various components of *q* (after Gkimprixis et al. 2019).

3 APPLICATION OF THE RTBF APPROACH FOR ITALY

This section employs the RTBF technique to derive example risk-targeted maps for Italy. The hazard input for the *PGA* is provided by Gruppo di Lavoro MPS (2004) for a 10%-in-50-years probability of exceedance (see Figure 3), while data for other probabilities of exceedance are available in Meletti and Montaldo (2007).

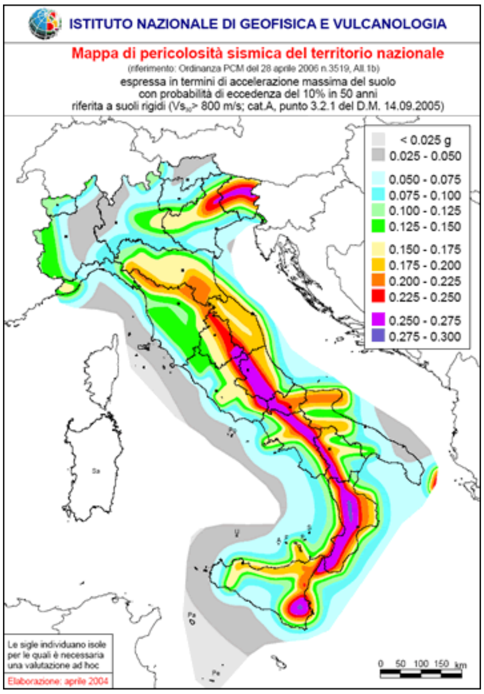

Figure 3. The Seismic Hazard Input for the *PGA* corresponding to a 10%-in-50-years probability of exceedance (after Gruppo di Lavoro MPS (2004).

In addition, the spectral acceleration values for a period of 0.5s are obtained from Montaldo and Meletti (2007). The target risk level is set equal to $2 \cdot 10^{-4}$ yrs^{-1}, a value proposed in ASCE 7-16 (2017), roughly corresponding to a 1% probability of exceedance in 50 years. The power law hazard model is fitted through two points (see Gkimprixis et al. 2019, paragraph 3.1). Based on the available data, the fitting points refer to a probability of exceedance in 50 years roughly equal to 2% and 10%.

Figure 4a and Figure 5a show the values of PGA^{ref} and $S_a^{ref}(T)$ according to PSHA and a reference return period of 475 years, whereas the values of k_1 corresponding to the slope of the fitted curve are plotted in Figure 4b an Figure 5b. A high variation of the slope of the hazard curve is observed. There are cases where the curve is quite steep with $k_1 > 5$, while other locations have hazard curves with very low slopes, for instance lower than 1.4.

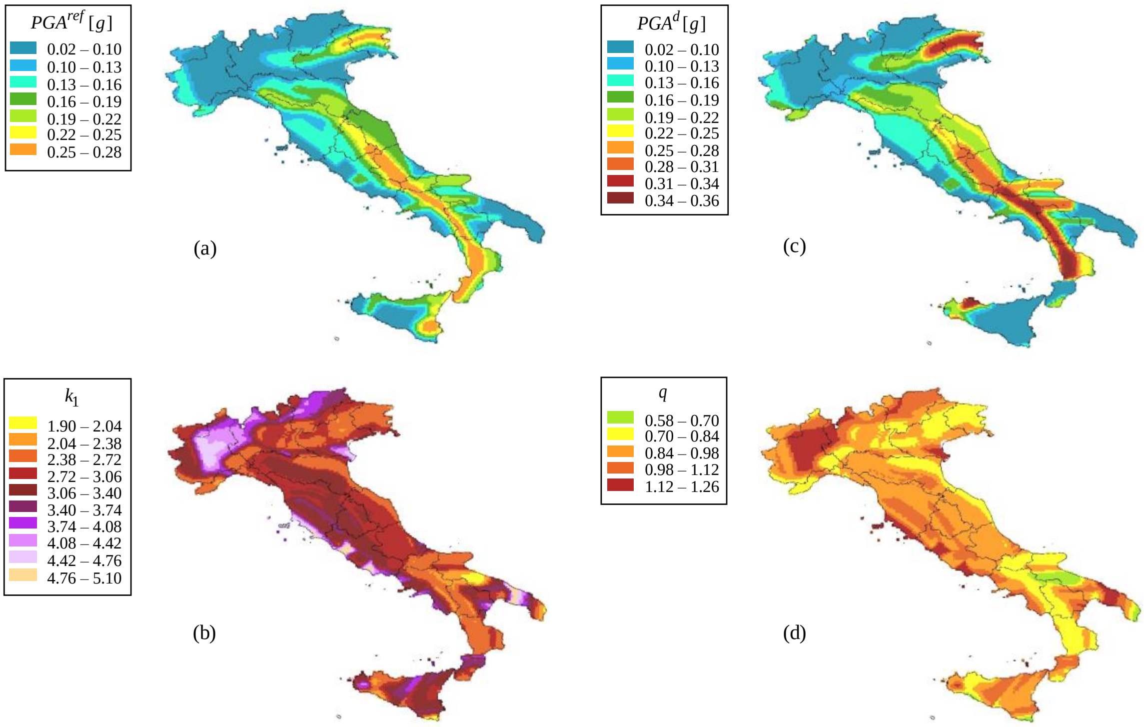

Figure 4. Seismic design maps for Italy in terms of *PGA*: (a) *PGA* at reference return period (475 years), (b) k_1 for the power-law approximation, (c) risk-targeted design *PGA* and (d) risk-targeted behaviour factor.

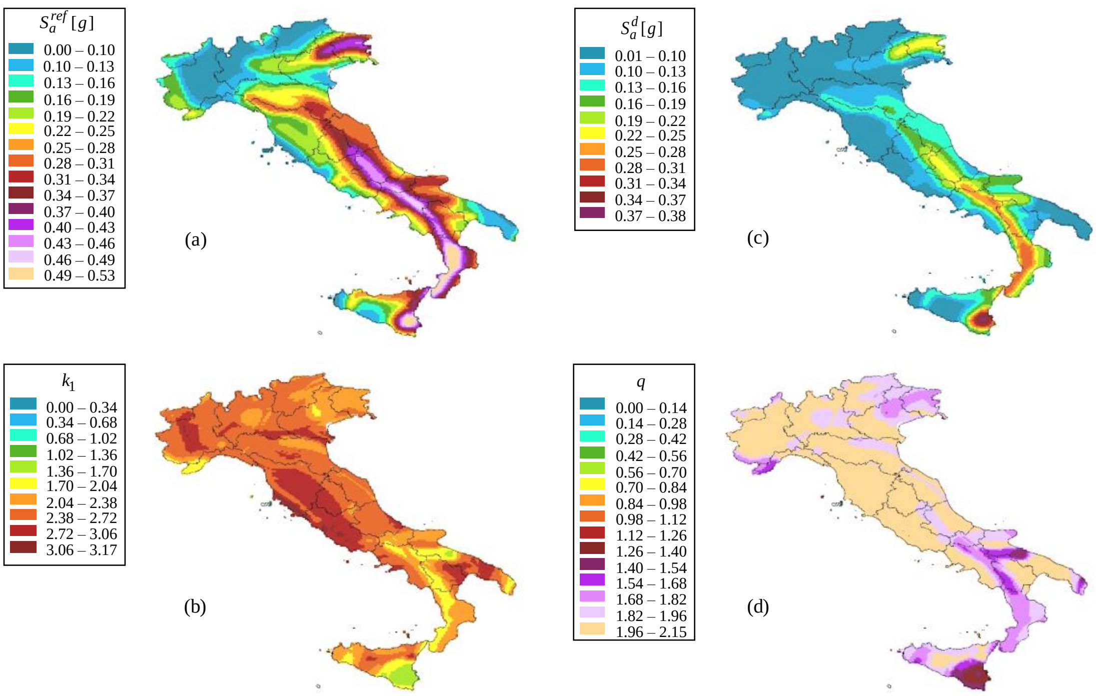

Figure 5. Seismic design maps for Italy in terms of S_a (T=0.5s): (a) Spectral acceleration for T=0.5s at reference return period (475 years), (b) k_1 for the power-law approximation, (c) risk-targeted design *PGA* and (d) risk-targeted behaviour factor.

Figure 4c and Figure 5c show the risk-targeted values of the design acceleration, evaluated via Equation (10). For the case of the PGA, $\beta = 0$ and $\hat{q}_{\mu_c} = 1$, whereas for S_a (T=0.5s), $\hat{q}_{\mu_c}$ is assumed equal to 4 and $\beta = 0.6$, as per ASCE 7-16 (2017). In both cases the contribution of overstrength is considered as well, by assuming $q_S = 2$.

The values of the risk-targeted behaviour factor *q* are given in Figure 4d and Figure 5d. This factor is derived by the ratio of the reference design acceleration and the risk-targeted design acceleration. A value higher than one means that the reference design acceleration should be decreased in order to satisfy the risk acceptance criteria.

In general, low values of *q* are obtained. Of course, this conclusion is sensitive to the assumptions made for the target risk level and the ductility and overstrength of the system. For the case of S_a(T=0.5s), *q* is in general between 1.25 to 2.15. For the *PGA* though, *q* is lower than one in most areas, which means that the reference *PGA* should be increased to achieve the target risk level.

4 CONCLUSIONS

It has been widely acknowledged that the philosophy of 'uniform hazard' for seismic design of structures leads to uncontrollable levels of risk. Thus, researchers currently focus on developing alternative techniques to achieve explicit control of the risk of failure. In this paper, the probabilistic framework developed by Kennedy and Short (1994) and Cornell (1996), leading to the definition of risk-targeted behaviour factors (RTBFs), is summarised and the presented analytical formulas are then used to derive risk-targeted maps for Italy.

Based on the assumptions made for the target risk level and the structural systems considered, it is found that the design *PGA* should be increased in most areas, compared to the uniform-hazard value corresponding to a return period T_R=475 yrs. On the other hand, the values of the design spectral acceleration can be significantly lower than the ones corresponding to T_R=475 yrs.

5 ACKNOWLEDGEMENTS

This article is based on a previous work of the authors (see Gkimprixis et 2019). Herein, the methodology is applied in Italy using a different hazard input that refers specifically to the assessed area.

REFERENCES

Altieri, D., Tubaldi, E., De Angelis, M., Patelli, E., Dall'Asta, A. (2018). Reliability-based optimal design of nonlinear viscous dampers for the seismic protection of structural systems, *Bulletin of Earthquake Engineering*, **16**(2), 963-982.

Aschheim, M. (2002). Seismic design based on the yield displacement, *Earthquake Spectra*, **18**(4), 581-600. doi: 10.1193/1.1516754.

Baker, J. W. (2015). Introduction to Probabilistic Seismic Hazard Analysis, White Paper Version 2.1, 77 pp.

Barbato, M., Tubaldi, E. (2013). A probabilistic performance-based approach for mitigating the seismic pounding risk between adjacent buildings, *Earthquake Engineering & Structural Dynamics*, **42**(8), 1203-1219.

Benjamin, J. R., and Cornell, C. A. (1970). Probability, statistics, and decision for civil engineers, McGraw-Hill, New York.

Castaldo, P., Amendola, G., Palazzo, B. (2017). Seismic fragility and reliability of structures isolated by friction pendulum devices: seismic reliability-based design (SRBD), *Earthquake Engineering & Structural Dynamics*, **46**(3), 425-446.

Cornell, C. A. (1996). Calculating building seismic performance reliability: a basis for multi-level design norms, *Proceedings of 11th World Conference on Earthquake Engineering*, Acapulco.

Cornell, C. A., Jalayer, F., Hamburger, R. O., Foutch, D. A. (2002). Probabilistic basis for 2000 SAC Federal Emergency Management Agency steel moment frame guidelines, *Journal of Structural Engineering*, **128**(4), 526-533.

Douglas, J., Gkimprixis, A. (2018). Risk targeting in seismic design codes: The state of the art, outstanding issues and possible paths forward, *Seismic Hazard and Risk Assessment - Updated Overview with Emphasis on Romania, R. Vacareanu and C. Ionescu (eds)*, Springer. https://doi.org/10.1007/978-3-319-74724-8_14.

Fajfar, P. (2018). Analysis in seismic provisions for buildings: past, present and future, *Bulletin of Earthquake Engineering*, **16**: 2567-2608, Springer, https://doi.org/10.1007/s10518-017-0290-8.

Fajfar, P., Dolšek, M. (2012). A practice-oriented estimation of the failure probability of building structures, *Earthquake Engineering & Structural Dynamics*, **41**(3), 531-547.

Fragiadakis, M., Papadrakakis, M. (2008). Performance-based optimum seismic design of reinforced concrete structures, *Earthquake Engineering & Structural Dynamics*, **37**(6), 825-844.

Franchin, P., Petrini, F., Mollaioli, F. (2018). Improved risk-targeted performance-based seismic design of reinforced concrete frame structures, *Earthquake Engineering & Structural Dynamics*, **47**(1), 49-67.

Gidaris, I., Taflanidis, A. A. (2015). Performance assessment and optimization of fluid viscous dampers through life-cycle cost criteria and comparison to alternative design approaches, *Bulletin of Earthquake Engineering*, **13**(4), 1003-1028.

Gkimprixis, A., Tubaldi, E. & Douglas, J. (2019). Comparison of methods to develop risk-targeted seismic design maps, *Bulletin of Earthquake Engineering*, **17**:

3727-3752. https://doi.org/10.1007/s10518-019-00629-w.
Gruppo di Lavoro MPS (2004). Redazione della mappa di pericolosità sismica prevista dall'Ordinanza PCM del 20 marzo 2003 n. 3274, All. 1. Rapporto conclusivo per il Dipartimento della Protezione Civile, aprile 2004, Istituto Nazionale di Geofisica e Vulcanologia (INGV), Milano-Roma, Italy, available at http://zonesismiche.mi.ingv.it/ (last accessed July 2019).
Iervolino, I., Spillatura, A., Bazzurro, P. (2017). RINTC project-assessing the (implicit) seismic risk of codeconforming structures in Italy, *COMPDYN 2017-6th ECCOMAS thematic conference on computational methods in structural dynamics and earthquake engineering*, Rhodes Island, Greece, pp 15–17.
Kappos, A. J. (1999). Evaluation of behavior factors on the basis of ductility and overstrength studies, *Engineering Structures*, **21**(9), 823-835.
Kennedy, R. P., Short, S. A. (1994). Basis for seismic provisions of DOE-STD-1020. Rep. No. UCRL-CR-111478, Lawrence Livermore National Laboratory, Livermore, Calif., and Rep. No. BNL-52418, Brookhaven National Laboratory, Upton, N.Y.
Luco, N., Bachman, R. E., Crouse, C. B., Harris, J. R., Hooper, J. D., Kircher, C. A., Caldwell P. J., Rukstales, K. S. (2015). Updates to Building-Code Maps for the 2015 NEHRP Recommended Seismic Provisions, *Earthquake Spectra*, **31**(S1), S245-S271.
Luco, N., Cornell, C. A. (2007). Structure-specific scalar intensity measures for near-source and ordinary earthquake ground motions, *Earthquake Spectra*, **23**(2):357–392.
Luco, N., Ellingwood, B. R., Hamburger, R. O., Hooper, J. D., Kimball, J. K., Kircher, C. A. (2007). Risk-targeted versus current seismic design maps for the conterminous United States. In: *SEAOC 2007 convention proceedings*.
Lupoi, G., Lupoi, A., Pinto, P. E. (2002). Seismic risk assessment of RC structures with the" 2000 SAC/FEMA" method, *Journal of Earthquake Engineering*, **6**(04), 499-512.
McGuire, R. K. (2008). Probabilistic seismic hazard analysis: early history, *Earthquake Engineering and Structural Dynamics*, **37:**329–338, doi: 10.1002/eqe.765.
Meletti C., Montaldo V., 2007. Stime di pericolosità sismica per diverse probabilità di superamento in 50 anni: valori di ag. Progetto DPC-INGV S1, Deliverable D2, http://esse1.mi.ingv.it/d2.html (last accessed July 2019).
Montaldo V., Meletti C., 2007. Valutazione del valore della ordinata spettrale a 1sec e ad altri periodi di interesse ingegneristico. Progetto DPC-INGV S1, Deliverable D3, http://esse1.mi.ingv.it/d3.html (last accessed July 2019).
Vamvatsikos, D. (2013). Derivation of new SAC/FEMA performance evaluation solutions with second-order hazard approximation, *Earthquake Engineering & Structural Dynamics*, **42**(8), 1171-1188.
Vamvatsikos, D., Aschheim, M. A. (2016). Performance-based seismic design via yield frequency spectra, *Earthquake Engineering & Structural Dynamics*, **45**(11), 1759-1778.
Žižmond, J., Dolšek, M. (2017). The formulation of risk-targeted behaviour factor and its application to reinforced concrete buildings, *Proceedings of 16th World Conference on Earthquake Engineering*, Paper no. 1659.